Open Research Online

The Open University's repository of research publications
and other research outputs

Proarrhythmic proclivity of left-stellate ganglion stimulation in a canine model of drug-induced long-QT syndrome type 1

Journal Item

How to cite:

ter Bekke, Rachel M. A.; Moers, Annerie M. E.; de Jong, Monique M. J.; Johnson, Daniel M.; Schwartz, Peter J.; Vanoli, Emilio and Volders, Paul G. A. (2019). Proarrhythmic proclivity of left-stellate ganglion stimulation in a canine model of drug-induced long-QT syndrome type 1. International Journal of Cardiology, 286 pp. 66–72.

For guidance on citations see FAQs.

© 2019 The Authors

Version: Version of Record

Link(s) to article on publisher's website:
http://dx.doi.org/doi:10.1016/j.ijcard.2019.01.098

Copyright and Moral Rights for the articles on this site are retained by the individual authors and/or other copyright owners. For more information on Open Research Online's data policy on reuse of materials please consult the policies page.

oro.open.ac.uk

International Journal of Cardiology 286 (2019) 66–72

Contents lists available at ScienceDirect

International Journal of Cardiology

journal homepage: www.elsevier.com/locate/ijcard

Proarrhythmic proclivity of left-stellate ganglion stimulation in a canine model of drug-induced long-QT syndrome type 1

Rachel M.A. ter Bekke [a,1], Annerie M.E. Moers [a,1], Monique M.J. de Jong [a,1], Daniel M. Johnson [a,1], Peter J. Schwartz [b,1], Emilio Vanoli [c,d,1], Paul G.A. Volders [a,*,1]

[a] Department of Cardiology, Cardiovascular Research Institute Maastricht (CARIM), Maastricht University Medical Center, Maastricht, the Netherlands
[b] Center for Cardiac Arrhythmias of Genetic Origin, IRCCS Istituto Auxologico Italiano, Milano, Italy
[c] Department of Molecular Medicine, University of Pavia, Pavia, Italy
[d] Cardiovascular Department IRCCS MultiMedica, Sesto san Giovanni

ARTICLE INFO

Article history:
Received 30 September 2018
Received in revised form 24 January 2019
Accepted 29 January 2019
Available online 31 January 2019

Keywords:
Long-QT syndrome
Ventricular arrhythmia
Autonomic nervous system
Torsades de pointes

ABSTRACT

Background: Left-stellate ganglion stimulation (LSGS) can modify regional dispersion of ventricular refractoriness, promote triggered activity, and reduce the threshold for ventricular fibrillation (VF). Sympathetic hyperactivity precipitates torsades de pointes (TdP) and VF in susceptible patients with long-QT syndrome type 1 (LQT1). We investigated the electromechanical effects of LSGS in a canine model of drug-induced LQT1, gaining novel arrhythmogenic insights.

Methods: In nine mongrel dogs, the left and right stellate ganglia were exposed for electrical stimulation. ECG, left- and right-ventricular endocardial monophasic action potentials (MAPs) and pressures (LVP, RVP) were recorded. The electromechanical window (EMW; Q to LVP at 90% relaxation minus QT interval) was calculated. LQT1 was mimicked by infusion of the KCNQ1/I_{Ks} blocker HMR1556.

Results: At baseline, LSGS and right-stellate ganglion stimulation (RSGS) caused similar heart-rate acceleration and QT shortening. Positive inotropic and lusitropic effects were more pronounced under LSGS than RSGS. I_{Ks} blockade prolonged QTc, triggered MAP-early afterdepolarizations (EADs) and rendered the EMW negative, but no ventricular tachyarrhythmias occurred. Superimposed LSGS exaggerated EMW negativity and evoked TdP in 5/9 dogs within 30 s. Preceding extrasystoles originated mostly from the outflow-tracts region. TdP deteriorated into therapy-refractory VF in 4/5 animals. RSGS did not provoke TdP/VF.

Conclusions: In this model of drug-induced LQT1, LSGS readily induced TdP and VF during repolarization prolongation and MAP-EAD generation, but only if EMW turned from positive to very negative. We postulate that altered mechano-electric coupling can exaggerate regional dispersion of refractoriness and facilitates ventricular ectopy.

© 2019 The Authors. Published by Elsevier B.V. This is an open access article under the CC BY-NC-ND license (http://creativecommons.org/licenses/by-nc-nd/4.0/).

1. Introduction

Stimulation of the left (LSGS) and right stellate ganglion (RSGS) has generalized cardiovascular (i.e., heart-rate and blood-pressure rise) and localized myocardial effects. Marked differences in chronotropic, inotropic, lusitropic, and dromotropic effects exist among species, including humans [1,2]. LSGS mainly causes electrical activation of the left-ventricular (LV) inferior and lateral regions, whereas RSGS modulates predominantly the anterior sides of both ventricles [3]. Sympathetic hyperactivity and/or regionally dispersed sympathetic innervation impinge on these electrophysiological properties [1], potentially exaggerating dispersion of excitation and refractoriness. Augmented LSG activity facilitates triggered activity [4], shortens ventricular refractoriness [5], and reduces the threshold for ventricular fibrillation (VF) in normal and structurally-remodeled hearts [6,7].

Sympathetic-related ventricular tachyarrhythmias are a hallmark of the long-QT syndrome type 1 (LQT1), as arrhythmic events are mostly evoked during exercise and/or emotion (~90% of symptomatic LQT1 patients) [8]. Accordingly, beta-adrenergic receptor blockade is the mainstay of therapy, and left-cardiac sympathetic denervation should be considered in symptomatic patients when beta-blockade is not effective, not tolerated or contraindicated [9–11].

Previous studies in canine LQTS models addressed the effects of unilateral or bilateral stellate ganglion stimulation during cesium-chloride-induced QT prolongation [12] and *d*-sotalol-induced LQT2 [13]. In drug-induced LQT1, TdP was readily evoked by the beta-adrenergic agonist isoproterenol [14]. In the latter, exaggerated spatiotemporal dispersion of repolarization, substantial electromechanical heterogeneities

* Corresponding author at: Department of Cardiology, CARIM, Maastricht University Medical Center, PO Box 5800, 6202 AZ Maastricht, the Netherlands.
E-mail address: p.volders@maastrichtuniversity.nl (P.G.A. Volders).
[1] This author takes responsibility for all aspects of the reliability and freedom from bias of the data presented and their discussed interpretation.

https://doi.org/10.1016/j.ijcard.2019.01.098
0167-5273/© 2019 The Authors. Published by Elsevier B.V. This is an open access article under the CC BY-NC-ND license (http://creativecommons.org/licenses/by-nc-nd/4.0/).

(e.g., a negative electromechanical window (EMW): duration of mechanical systole minus electrical systole) and postsystolic aftercontractions heralded TdP, suggesting proarrhythmic contributions of mechano-electric feedback [14]. Related to this, EMW negativity was a strong indicator of arrhythmic risk in LQT1 patients [15].

To date, no study has addressed ventricular electromechanical relations during sympathetic-evoked arrhythmias in LQT1. We applied LSGS and RSGS to unmask ventricular arrhythmogenic mechanisms in the anesthetized canine model of drug-induced LQT1 [14]. Electrical stimulation of the LSG and RSG was performed with sympathetic and vagal nerves left intact, during an anesthetic regime with minimal influence on beta-adrenergic responsiveness and baroreflex sensitivity, allowing near-to-normal autonomic reflexes during sympathetic stimulation. Simultaneous recordings of ECGs, monophasic action potentials (MAPs) and pressures from the left (LVP) and right ventricle (RVP) served to examine electromechanical coupling during stellate-ganglion stimulation.

2. Methods

Animal handling was in accordance with the Dutch Law on Animal Experimentation and the European Directive for the Protection of Vertebrate Animals used for experimental and other scientific purposes (European Union Directive 86/609/CEE). The Committee for Experiments on Animals of Maastricht University approved the experimental protocol (2008–116).

2.1. General

Nine adult mongrel dogs of either sex (body weight 32 ± 3 kg, Marshall BioResources) were used for this study. Food was withheld 12 h before the experiment. General anesthesia was induced by a slow singular intravenous injection of remifentanil (0.1 μg/kg), etomidate (0.5–1.5 mg/kg), and succinylcholine (1 mg/kg). A cuffed endotracheal tube was inserted and connected to a respirator with 30% oxygen in pressurized air to maintain normocapnia, $PaCO_2$ 30–50 mm Hg. A thermal mattress was used to maintain body temperature and 1.25 mL/kg/h 0.9% NaCl was administered to compensate for the perioperative fluid loss. Anticoagulation was achieved with 500 IU/kg unfractionated heparin. During the experiment, anesthesia was maintained by continuous infusion of etomidate (1.0–3.0 mg/kg/h) and remifentanil (0.6–1.0 μg/kg/min). This anesthetic regime was chosen because of minimal effects on beta-adrenergic responsiveness, baroreflex sensitivity, and basal hemodynamic parameters [14,16,17].

2.2. In-vivo experimental design

In all experiments standard-lead ECGs were continuously registered. Additionally, MAP catheters (Hugo Sachs Elektronik, Harvard Bioscience, Inc.) were positioned in the LV and RV. Endocardial MAP signals were accepted on the basis of amplitude, morphology and stability. Two 7F pigtail tip-micromanometer catheters (Sentron, Cordis®) were advanced via arterial and venous (femoral or carotid) access into the LV and RV cavity for pressure recordings.

In all dogs, the left cardiac sympathetic chain was exposed beneath the parietal pleura by left thoracotomy between the first and second ribs, posteriorly. In three dogs, the contralateral stellate ganglion was also exposed and prepared for electrical stimulation. The vagal nerves were left intact and sympathetic neural decentralization was not performed. Custom-made bipolar electrodes were used for unilateral stellate stimulations. Pulses generated were 2–4 mA in amplitude, 2 ms in duration, 10–15 Hz in frequency [1,3,6,13], and were maintained for 33 ± 12 s. The frequency of stimulation was chosen to mimic the spontaneous firing rate in efferent cardiac sympathetic nerves during a physiological reflex (Online Fig. 1) [18]. If both sympathetic stellate ganglia were to be stimulated in an experiment, the RSG was stimulated first. The aim of our experiments was to investigate the arrhythmogenic mechanisms during LSGS-evoked ventricular arrhythmias; RSGS was performed only to confirm known physiological responses. At least 5 min between successive stimulations were allowed for full recovery of the nerve, and hemodynamic and electrophysiological parameters.

Once a reproducible response to either stellate ganglion was established in at least two consecutive stimulations, HMR1556, an I_{Ks} blocker targeting KCNQ1 [19], was administered intravenously at 25–50 μg/kg/min (mean 46 ± 10 μg/kg/min) to mimic LQT1. HMR1556 was titrated to reach maximal I_{Ks} inhibition, as assessed by stable QT prolongation >25% from baseline [14], before stellate ganglion stimulation was repeated. If TdP or VF was induced, electrical stimulation and HMR1556 infusion were discontinued immediately, followed by magnesium administration and external electrical cardioversion in attempts to restore sinus rhythm.

2.3. Data analysis

Electrophysiological, hemodynamic and electromechanical parameters described below were analyzed during ten consecutive sinus-rhythm (or supraventricular) beats, momentarily before and at maximal SGS, both under baseline conditions and during I_{Ks} blockade.

Heart rate and QT interval were measured from an extremity lead (usually lead II) with a discernible T-wave ending and the longest QT interval. Heart-rate corrected QT (QTc) was calculated using van de Water's formula, QTc = QT-0.087(RR-1000), which is superior to Bazett's in anesthetized dogs [20]. T_{peak}-T_{end} was calculated as a marker of spatial dispersion of ventricular repolarization.

LV and RV MAP durations were measured at 90% repolarization ($MAPD_{90}$). Beat-to-beat variability of repolarization was measured on LV and RV MAP recordings during 10 consecutive beats in the absence of ventricular ectopy. Short-term variability was calculated as: $STV = \sum(|MAPD_n\text{-}MAPD_{n-1}|)/(10^*\sqrt{2})$. Long-term variability as: $LTV = \sum(|MAPD_n + MAPD_{n-1}\text{-}2^*MAPD_{mean}|)/(10^*\sqrt{2})$ [21]. Also, the occurrence of early afterdepolarizations (EADs) in MAPs, and EAD-preceding transient repolarization delays (i.e., when dV_{MAP}/dt turned less negative or zero) were noted.

Ventricular peak systolic and end-diastolic pressure, duration of ventricular contraction at 90% relaxation ($QLVP_{90}$), and the dP/dt_{max}, dP/dt_{min} were measured. The EMW was calculated by subtracting the QT interval from the $QLVP_{90}$. The pressure signals were carefully screened for (low-amplitude) aftercontractions [14].

If ventricular tachyarrhythmia occurred, we located the origin of the triggering premature ventricular complex (PVC) by analyzing the QRS morphology and the sequence of RV and LV MAP activation. The last supraventricular beat before TdP/VF was designated beat "0" with the preceding intervals being $I_{(-n)}$ (Online Fig. 2). These RR intervals were measured to determine the pause dependency of arrhythmia initiation, defined as $I_{(-1)} \geq 150\%\ I_{(-2)}$ [22]. QT, EMW, and $QLVP_{90}$ were compared between TdP-inducible and noninducible stimulations. Dogs were designated "resistant" if no TdP/VF could be induced during SGS.

2.4. Statistical analysis

Data were measured in 10 consecutive beats, using the average for further statistical analysis. Pooled data were expressed as mean ± standard deviation. Normality was assessed for each dataset using the Shapiro-Wilk test. Differences of parameters in paired data were assessed using the paired-samples *t*-test or the Wilcoxon signed rank test as appropriate. Intergroup comparison was performed using the Student's t-test or the Kruskal-Wallis test. A *P* value of <0.05 was considered statistically significant.

3. Results

3.1. Stellate ganglion stimulation of the normal canine heart

Fig. 1 depicts representative examples of the cardiac effects of LSGS and RSGS at baseline. During LSGS, heart rate increased by 79% and the QT interval shortened by 23%, effectively reducing QTc from 290 ± 24 to 253 ± 13 ms ($P = 0.0003$; Online Table 1). LV and RV $MAPD_{90}$ analysis did not reveal augmented interventricular or temporal (i.e., beat-to-beat) dispersion of repolarization. In both ventricles, inotropy increased significantly: LV peak systolic pressure by 37% and RVP by 157%. LV dP/dt_{max} increased by 394%. LV dP/dt_{min} decreased by 110%, indicating increased lusitropy, and effectively leading $QLVP_{90}$ to shorten from 373 ± 65 to 214 ± 46 ms (−43%, $P = 0.006$; Online Table 1). Changes in diastolic LVP did not reach statistical significance. Due to preferential mechanical-systole over QT shortening, LV EMW decreased from 95 ± 53 to 9 ± 42 ms ($P = 0.009$, Fig. 2). RV inotropy and lusitropy also increased significantly (Online Table 1).

LSGS readily evoked a junctional or low-atrial tachycardia, overriding the LSGS-induced accelerated sinus rhythm within 6 ± 3 s (asterisks in Fig. 1). Occasionally, solitary RV/LV ectopic activity occurred during LSGS, but MAP-EADs, aftercontractions, or (non)sustained ventricular tachyarrhythmias (NSVT) were not observed. In approximately one third of LSG stimulations a short-lived paradoxical heart-rate slowing was observed, which could be counteracted by atropine.

We observed an immediate and protracted (87 ± 41 s) vagal rebound following LSGS (Fig. 3) characterized by sinus bradycardia, ventricular ectopy, and episodes of idioventricular rhythm. The post-LSGS systolic LVP remained elevated during this vagal episode, and returned to steady-state values parallel with the restoration of sinus rhythm. Such vagal rebound was never observed after isoproterenol administration in the same experimental set-up [14].

RSGS (n = 3, Fig. 1) caused comparable heart-rate accelerations (188 ± 55 bpm) as LSGS (in the absence of decentralization), without provoking supraventricular arrhythmias. Both QT and QTc intervals shortened significantly (by 29% and 18% respectively), but these were not different from the effects of LSGS. Endocardial $MAPD_{90}$ decreased

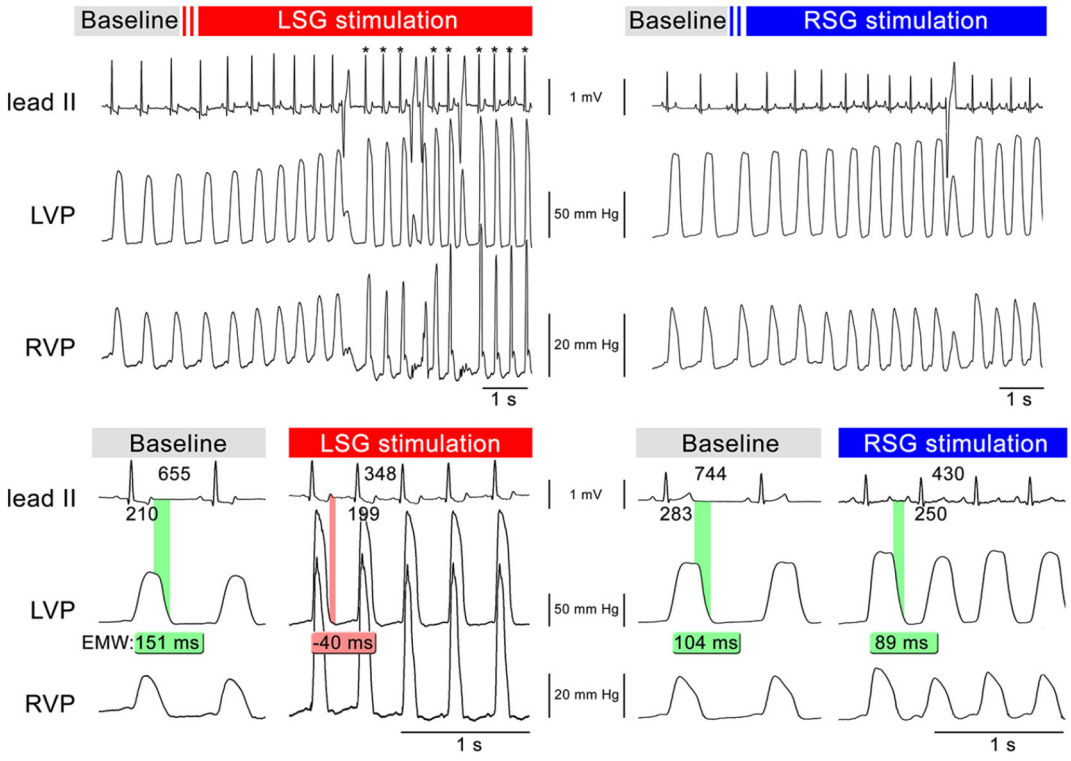

Fig. 1. Representative examples of effects of LSGS and RSGS on ECG, LVP, and RVP characteristics. Upon LSGS, a junctional tachycardia appeared after 6 s (*), which was interspersed by ventricular extrasystoles. The EMW, being positive at baseline, turned negative during LSGS (−40 ms, red), but not during RSGS (89 ms, green). LSG indicates left-stellate ganglion; RSG, right stellate ganglion; EMW, electromechanical window; LVP, left-ventricular pressure; RVP, right-ventricular pressure.

similarly in both ventricles (Online Table 1). RSGS-evoked positive inotropy was less prominent than during LSGS. Similarly, we observed only limited $QLVP_{90}$ shortening upon RSGS, resulting in less EMW reduction than upon LSGS (Online Table 1).

3.2. Repolarization instability during I_{Ks} inhibition

Intravenous administration of HMR1556 prolonged QT and QTc to 373 ± 65 and 371 ± 61 ms, respectively (+21% and + 20%; $P = 0.002$ and $P = 0.007$, Table 1). Heart rate decreased to 60 ± 11 bpm ($P = 0.0003$). Preferential LV over RV $MAPD_{90}$ prolongation (335 ± 74 and 286 ± 50 ms; $P < 0.0001$) augmented interventricular dispersion of repolarization. This was paralleled by a more pronounced LV temporal dispersion of repolarization, with $STV\text{-}MAPD_{90}$ increasing by 129% and $LTV\text{-}MAPD_{90}$ by 173%. LV EADs emerged in four dogs at a wide range of cycle lengths; RV EADs in three dogs (Fig. 4). Upon I_{Ks} inhibition, the LV-peak systolic pressure and LV dP/dt_{max} increased to 114 ± 19 mm Hg (+23%; $P = 0.01$) and 2373 ± 1159 mm Hg/s (+27%; $P = 0.001$). Despite a significant prolongation of the electrical systole, $QLVP_{90}$ remained unaltered, providing an EMW negativity of −14 ± 69 ms ($P = 0.001$, Fig. 2). No sizeable aftercontractions or spontaneous ventricular arrhythmias occurred under these conditions.

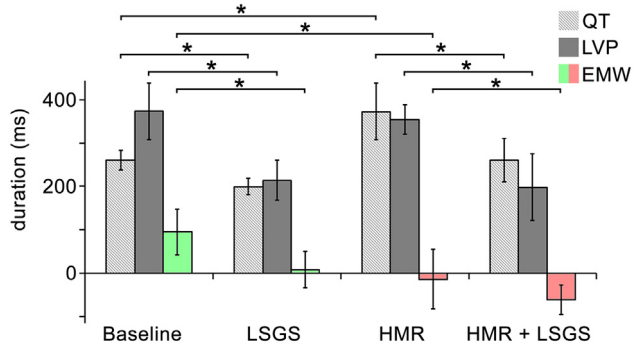

Fig. 2. Bar graph demonstrating the mean QT, QLVP, and EMW changes after LSGS, HMR1556, and LSGS during I_{Ks} inhibition. * $P < 0.05$. Abbreviations as in Fig. 1.

3.3. Proarrhythmic proclivity of LSGS during drug-induced LQT1

Left-sided sympathetic stimulation during I_{Ks} inhibition led to QTc and APD_{90} shortening to 306 ± 44 ms and 225 ± 31 ms respectively (Table 1). A markedly decreased $QLVP_{90}$ rendered the EMW negative (−61 ± 34 ms; $P = 0.0004$, Fig. 2). Beat-to-beat variability of repolarization duration increased and T-wave amplitudes reduced. Under these conditions, TdP/VF occurred in 5 of 9 dogs after 26 ± 6 s (Fig. 5). In most animals, once TdP initiated it rapidly degenerated into VF that did not respond to immediate and repeated electrical cardioversion, and was resistant to magnesium infusion. In one dog, a protracted vagal period with intermittent episodes of nonsustained VT was observed after termination of VF. RSGS was never torsadogenic.

In the dogs with inducible TdP/VF, pre-LSGS QT was significantly more prolonged and LV EMW more negative than in resistant animals: 440 ± 67 versus 344 ± 56 ms ($P = 0.007$) and −64 ± 87 versus 27 ± 40 ms ($P = 0.04$), respectively (Fig. 6). EMW negativity was more pronounced in the final beats preceding TdP/VF (reaching −94 ± 31 ms at $I_{(0)}$), compared with the non-inducible group (−43 ± 25 ms; $P = 0.002$, Figs. 5 and 6). $QLVP_{90}$ did not differ between these groups. QT prolongation was more exaggerated (282 ± 53 ms; $P = 0.02$) in the beats prior to TdP when compared to pre-NSVT (225 ± 21 ms) or solitary PVCs (229 ± 39 ms) in susceptible animals, and EMW was more negative −94 ± 31 ms prior to TdP/VF ($P = 0.005$) versus −23 ± 37 ms (pre-NSVT), and −38 ± 37 ms (pre-PVC).

An initial delay in MAP repolarization was present throughout a broad range of RR cycle lengths during LSGS and I_{Ks} blockade, but

Table 1
Electrophysiological and hemodynamic effects of HMR1556 and unilateral stellate ganglion stimulation.

	Baseline	HMR	*P* value	+ LSGS	*P* value	+ RSGS	*P* value
RR interval (ms)	680 ± 116	1026 ± 168	0.0002	481 ± 184	<0.0001	407 ± 82	0.02
Heart rate (bpm)	91 ± 17	60 ± 11	0.0003	142 ± 48	<0.0001	152 ± 30	0.01
QT interval (ms)	280 ± 23	373 ± 65	0.002	260 ± 50	<0.0001	246 ± 37	0.005
QTc (ms)	308 ± 17	371 ± 61	0.007	306 ± 44	<0.0001	298 ± 34	0.003
Tp-Te (ms)	57 ± 27	92 ± 34	0.03	47 ± 16	<0.0001	44 ± 10	0.007
Left ventricle							
$MAPD_{90}$ (ms)	238 ± 29	335 ± 74	0.001	225 ± 31	0.001	230 ± 58	0.14
MAP-STV	2.8 ± 1.6	6.4 ± 4.6	0.003	6.1 ± 3.9	0.08	8.9 ± 11.3	0.76
MAP-LTV	3.3 ± 1.5	9.0 ± 8.1	0.02	10.2 ± 10.0	0.42	7.3 ± 9.2	0.86
LVP syst. (mm Hg)	102 ± 24	114 ± 19	0.01	180 ± 22	<0.0001	150 ± 27	0.0003
LVP diast. (mm Hg)	12 ± 8	14 ± 8	0.003	5 ± 8	0.003	16 ± 14	0.35
dP/dt_{max} (mm Hg/s)	1734 ± 857	2373 ± 1159	0.001	9267 ± 3498	<0.0001	3556 ± 1615	0.02
dP/dt_{min} (mm Hg/s)	−3127 ± 2634	−4432 ± 3466	0.07	−8774 ± 7044	0.0004	−3025 ± 1063	0.04
$QLVP_{90}$ (ms)	360 ± 31	355 ± 34	0.86	198 ± 77	0.0002	248 ± 45	0.002
EMW (ms)	79 ± 36	−14 ± 69	0.001	−61 ± 34	0.0004	11 ± 31	0.81
Right ventricle							
$MAPD_{90}$ (ms)	213 ± 21	286 ± 50	0.008	209 ± 52	<0.0001	204 ± 33	0.03
RVP syst. (mm Hg)	25 ± 9	28 ± 8	0.03	64 ± 16	0.003	35 ± 4	0.0002
RVP diast. (mm Hg)	6 ± 4	8 ± 5	0.02	7 ± 5	0.05	6 ± 6	0.03
dP/dt_{max} (mm Hg/s)	610 ± 316	820 ± 641	0.13	4635 ± 1526	0.005	929 ± 309	0.03
dP/dt_{min} (mm Hg/s)	−266 ± 47	−329 ± 39	0.02	−3290 ± 4983	0.008	−483 ± 150	0.12

STV indicates short-term variability; LTV, long-term variability; $MAPD_{90}$, monophasic action potential duration at 90% repolarization; LVP, left-ventricular pressure; $QLVP_{90}$, time from QRS onset to 90% LV pressure normalization; EMW, electromechanical window.

overt EADs did not occur (Fig. 4). Increased diastolic slopes suggesting delayed afterdepolarizations were also not observed. During this condition with fast-rate dependent electrical instability and mechano-electric heterogeneity, relatively short-coupled non-pause dependent PVCs occurred (Figs. 5–7). Macroscopic aftercontractions preceded TdP in one dog. The TdP/VF-triggering PVCs typically had an intermediate QRS axis, large QRS amplitudes, and their earliest endocardial activation at the RV MAP signal (in 4/5 dogs, Fig. 7), suggesting focal activation in the vicinity of the outflow-tracts region. In one animal, TdP initiation emerged from the inferior LV. TdP onset was non-pause dependent with $I_{(-1)}$ never exceeding $I_{(-2)}$. In some cases ventricular ectopy occurred prior to $I_{(-2)}$.

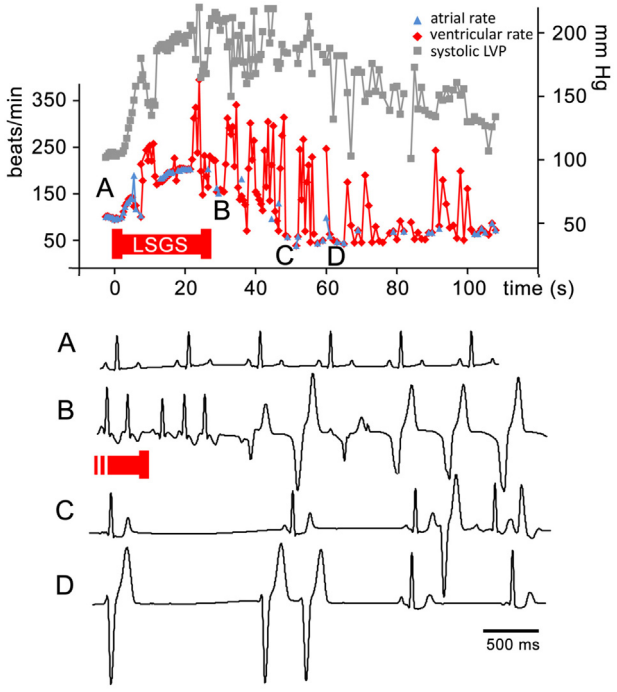

Fig. 3. Vagal rebound post-LSGS at baseline. Upon termination of LSGS, and during a protracted positive inotropic response (upper panel), sinus and junctional bradycardia, ventricular extrasystoles and idioventricular rhythm occurred, indicating a vagal response by a baroreflex loop and/or sympathetic withdrawal. The lower ECG traces A, B, C, and D are ECG examples at different stages of the vagal rebound. LVP indicates left-ventricular pressure.

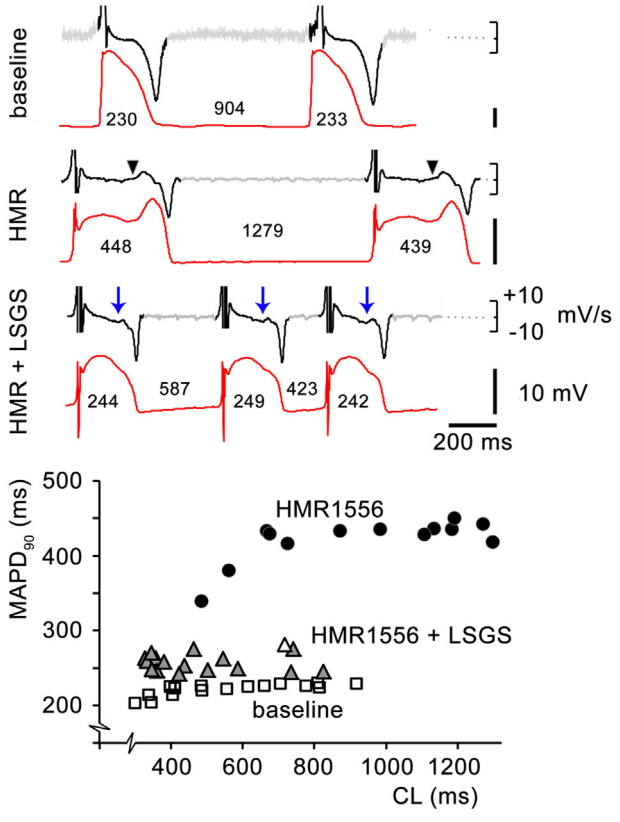

Fig. 4. Top, LV MAPs and first derivative (dV/dt) of MAP signal. After HMR1556, EADs followed after an initial delay in repolarization (arrowheads). Upon concomitant LSGS at 10–15 Hz, frank EAD upstrokes were absent but a discernable delay in repolarization (arrows) remained present, contributing to $MAPD_{90}$ prolongation. Bottom, rate dependency of $MAPD_{90}$ at baseline (square), during HMR1556 (circle) and simultaneous LSGS (triangle). Black symbols: EAD present; gray symbols: initial delay in repolarization. LSGS indicates left-stellate ganglion stimulation; APD_{90}, action potential duration at 90% repolarization; CL, cycle length.

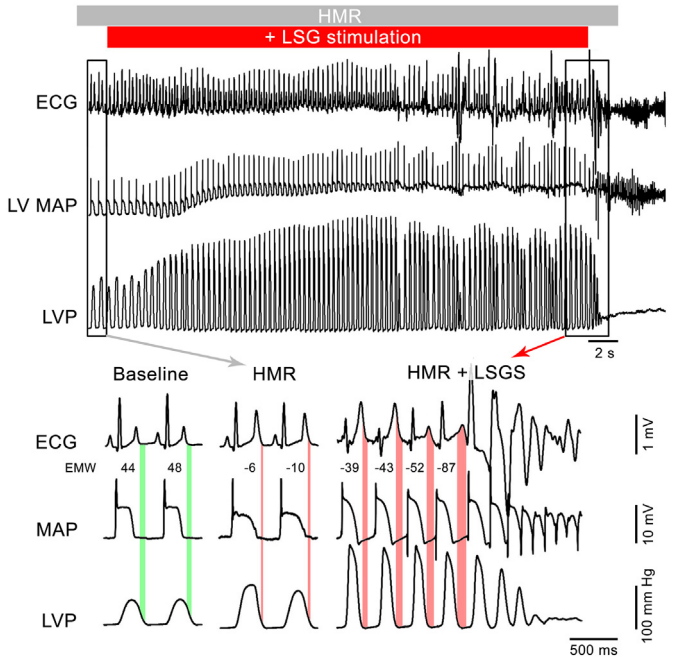

Fig. 5. Induction of TdP, degenerating into VF, after a short-coupled non-pause dependent PVC during LSGS in drug-induced LQT1. Abbreviations as in Fig. 1.

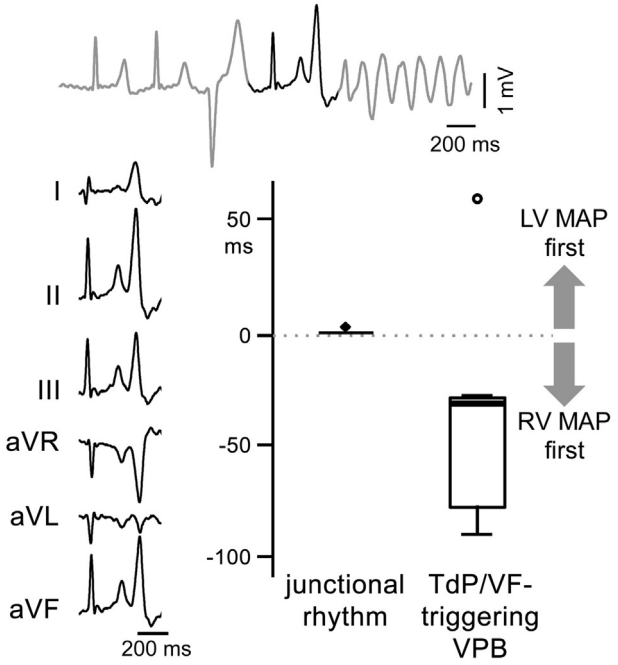

Fig. 7. Outflow-tract origins of TdP/VF-triggering (non-pause dependent) PVC. Left, 6-lead ECG recording showing an intermediate QRS axis with a relatively short duration. Right, box plot of interventricular activation delay of the junctional beats versus the TdP/VF-triggering extrasystoles demonstrating the earliest electrical activation in the RV in all but one case.

4. Discussion

This is the first study to demonstrate the proarrhythmic consequences of LSGS in an in-vivo model of drug-induced LQT1 [14] in which autonomic reflexes, neurocardiac transmission and cardiac electromechanical coupling are only mildly influenced by the applied anesthesia. In-vivo I_{Ks} blockade prolonged ventricular repolarization duration and augmented spatial and temporal repolarization dispersion, recapitulating LQT1 aspects. Only with concomitant LSGS did TdP occur, despite global repolarization shortening. Arrhythmia initiation was always fast-rate (non-pause) dependent [22,23], with the majority

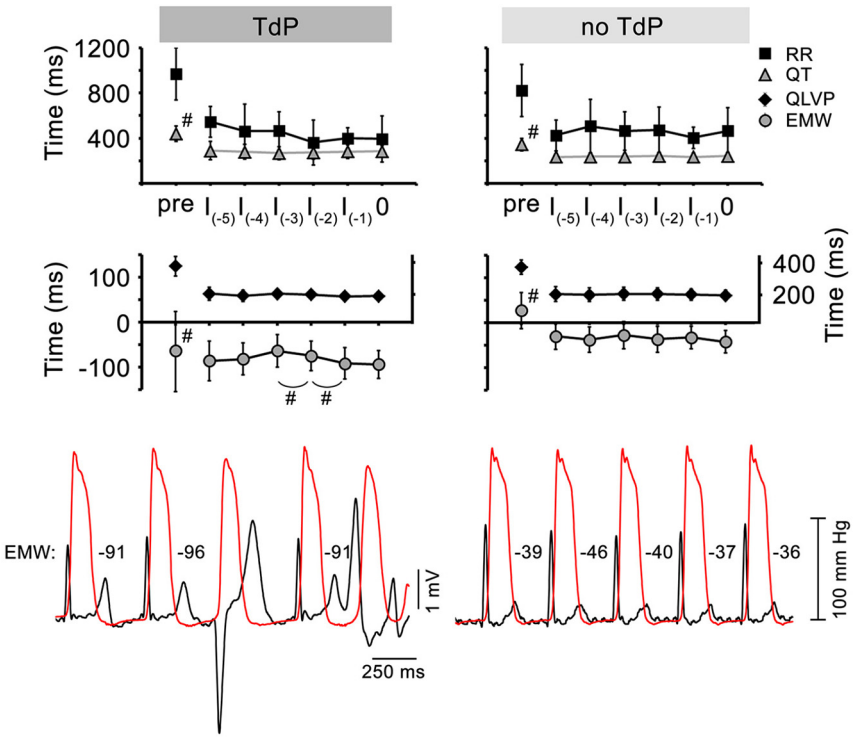

Fig. 6. Top, beat-to-beat changes in RR interval, QT interval, $QLVP_{90}$, and EMW during HMR1556 and LSGS just prior to TdP (left) or at 26 s and maximal chronotropic response (no TdP; right). Pre-LSGS QT and EMW were significantly more pronounced in TdP-susceptible animals. TdP initiation was fast-rate dependent due to short-coupled non-pause dependent PVCs. # indicates $P < 0.05$. Below, simultaneous recording of ECG lead II and LVP to illustrate EMW variations.

of triggering beats originating in the vicinity of the outflow-tracts region. This is consistent with the site of TdP onset in the majority of LQTS patients [24].

In this model of drug-induced LQT1, the finding of LSGS-induced repolarization shortening suggests that intense sympathetic stimulation can enhance residual I_{Ks} despite pharmacological inhibition. Other cesium-chloride-induced LQTS models with sympathetic stimulation led to similar results [12,25]. Inotropic and particularly lusitropic influences were dominant during left-sided stimulation. Therefore, mechanical systole shortened, and in the face of regional repolarization prolongation by I_{Ks} inhibition alone, superimposed LSGS exaggerated EMW disparity (Fig. 2), especially just prior to TdP. In most susceptible dogs with drug-induced LQT1 and LSGS, TdP rapidly deteriorated into defibrillation-resistant VF. Pronounced EMW negativity related to torsadogenesis has also been observed during beta-adrenergic stimulation in experimental LQT1 [17] and in clinical studies on symptomatic patients with genetically-confirmed LQTS [15,26]. This suggests that LSGS imposes regional electromechanical heterogeneities that facilitate arrhythmia during I_{Ks} inhibition/loss of function. In the present experiments, macroscopic aftercontractions were infrequently observed, but we speculate that the local myocardial effects of LSGS could have produced low-amplitude aftercontractile events (below the radar of global intracavitary pressure) with similar arrhythmogenic significance during EMW negativity. Future studies could focus on examining mechano-electric triggers of arrhythmia in LQTS.

4.1. Proarrhythmic proclivity of LSGS during I_{Ks} inhibition

The present findings confirm the arrhythmogenic role of left-sided cardiac sympathetic hyperactivity in a clinically-relevant LQT1 model. Sympathetically-induced TdP/VF was markedly resistant to defibrillation attempts. Sympathetic hyperactivity, releasing norepinephrine locally at the myocardial nerve endings, accentuates heterogeneity in ventricular repolarization under these conditions, and favors reentrant excitation, whereas circulating catecholamines or infused (nor)epinephrine act more uniformly [27]. These differences are accompanied by a considerably larger positive inotropic (but similar chronotropic) response upon LSGS followed by a protracted vagal rebound. This vagal accentuation could be explained by the sudden sympathetic withdrawal and/or by baroreflex activation in response to the elevated arterial pressures. Supported by the observation of a prominent vagal rebound in the rare case of successful cardioversion of VF, our results suggest that reflex vagal activation may have promoted the LQT1-related TdP to deteriorate into VF. Vagal nerve stimulation operates mainly by antagonizing cardiac sympathetic activity, but it also increases ventricular dispersion of repolarization, as demonstrated in the setting of drug-induced LQT2 [28]. Moreover, when applied during induced VF in pigs or sheep, vagal nerve stimulation increases the variability of the dominant VF frequency, potentially sustaining the arrhythmia [29].

The triggers for life-threatening events in most LQT1 patients are either physical (75%) or emotional stress (15%) while rest/sleep accounts for only 10% [8]. One third of patients have events during swimming [8]. These arrhythmias are effectively prevented in most LQT1 patients by beta-blockade or by left-cardiac sympathetic denervation [9,30]. On the other hand, strong vagal reflexes have been implicated in high-risk LQT1 patients [31,32], and cold-water submersion and swimming, a genotype-specific trigger, provokes powerful co-stimulation of both sympathetic and parasympathetic limbs, at least in the first instances [33]. Our experimental results do not allow firm conclusions on the contribution of vagal stimulation to ventricular proarrhythmia in LQTS, but they lend indirect support to the concept of "autonomic conflict" [34], which indicates that a more convoluted vago-sympathetic interaction can facilitate ventricular tachyarrhythmia.

4.2. Limitations

The present study involved a relatively small number of animals, which was driven by ethical considerations. However, the differences in results obtained in paired analysis or group comparisons were so profound that they readily reached statistical significance.

The use of an anesthesia model always brings into question the cardiovascular and autonomic effects of anesthesia, especially when dealing with autonomic interventions. In the present study, we minimized potentially confounding effects [16,17] by the choice of anesthetics.

5. Conclusions

For the first time in an in-vivo model of drug-induced LQT1, we demonstrate the arrhythmogenic potency of LSGS to induce TdP and VF during repolarization prolongation, MAP-EADs generation, exaggerated spatiotemporal dispersion of repolarization, and EMW negativity. LSGS always rendered the EMW more negative prior to arrhythmia induction, which suggests that altered mechano-electric coupling is somehow involved in the proarrhythmic proclivity. Triggering PVCs most often emerged from the LV and RV outflow-tract regions. Our results offer novel mechanistic understanding of LQT1-related arrhythmogenesis and strengthen the rationale for left-cardiac sympathetic denervation in the prevention of life-threatening arrhythmias in several cardiac disorders, ranging from channelopathies [10] to structural heart diseases [10,11].

Funding

P.G.A.V. was supported by a Vidi grant from the Netherlands Organization for Scientific Research (ZonMw 91710365).

Conflict of interest

None declared by all authors.

Acknowledgements

The authors wish to thank Roel L.H.M.G. Spätjens BSc, Maastricht University Medical Center, The Netherlands for excellent graphical support, and Antonio Zaza, MD, University of Milano Bicocca, Italy for fruitful discussions on neurocardiac physiology.

Appendix A. Supplementary data

Supplementary data to this article can be found online at https://doi.org/10.1016/j.ijcard.2019.01.098.

References

[1] T. Opthof, A.R. Misier, R. Coronel, J.T. Vermeulen, H.J. Verberne, R.G. Frank, A.C. Moulijn, F.J. van Capelle, M.J. Janse, Dispersion of refractoriness in canine ventricular myocardium. Effects of sympathetic stimulation, Circ. Res. 68 (1991) 1204–1215.
[2] J.L. Ardell, M.C. Andresen, J.A. Armour, G.E. Billman, P.S. Chen, R.D. Foreman, N. Herring, D.S. O'Leary, H.N. Sabbah, H.D. Schultz, K. Sunagawa, I.H. Zucker, Translational neurocardiology: preclinical models and cardioneural integrative aspects, J. Physiol. 594 (2016) 3877–3909.
[3] F. Yanowitz, J.B. Preston, J.A. Abildskov, Functional distribution of right and left stellate innervation to the ventricles. Production of neurogenic electrocardiographic changes by unilateral alteration of sympathetic tone, Circ. Res. 18 (1966) 416–428.
[4] P.G. Volders, M.A. Vos, B. Szabo, K.R. Sipido, S.H. de Groot, A.P. Gorgels, H.J. Wellens, R. Lazzara, Progress in the understanding of cardiac early afterdepolarizations and torsades de pointes: time to revise current concepts, Cardiovasc. Res. 46 (2000) 376–392.
[5] P.J. Schwartz, R.L. Verrier, B. Lown, Effect of stellectomy and vagotomy on ventricular refractoriness in dogs, Circ. Res. 40 (1977) 536–540.
[6] P.J. Schwartz, N.G. Snebold, A.M. Brown, Effects of unilateral cardiac sympathetic denervation on the ventricular fibrillation threshold, Am. J. Cardiol. 37 (1976) 1034–1040.

[7] S. Zhou, B.C. Jung, A.Y. Tan, V.Q. Trang, G. Gholmieh, S.W. Han, S.F. Lin, M.C. Fishbein, P.S. Chen, L.S. Chen, Spontaneous stellate ganglion nerve activity and ventricular arrhythmia in a canine model of sudden death, Heart Rhythm. 5 (2008) 131–139.
[8] P.J. Schwartz, S.G. Priori, C. Spazzolini, et al., Genotype-phenotype correlation in the long-QT syndrome: gene-specific triggers for life-threatening arrhythmias, Circulation 103 (2001) 89–95.
[9] P.J. Schwartz, M.J. Ackerman, The long QT syndrome: a transatlantic clinical approach to diagnosis and therapy, Eur. Heart J. 34 (2013) 3109–3116.
[10] P.J. Schwartz, Cardiac sympathetic denervation to prevent life-threatening arrhythmias, Nat. Rev. Cardiol. 11 (2014) 346–353.
[11] P.J. Schwartz, G.M. De Ferrari, L. Pugliese, Cardiac sympathetic denervation 100 years later: Jonnesco would have never believed it, Int. J. Cardiol. 237 (2017) 25–28.
[12] J. Ben-David, D.P. Zipes, Differential response to right and left ansae subclaviae stimulation of early afterdepolarizations and ventricular tachycardia induced by cesium in dogs, Circulation 78 (1988) 1241–1250.
[13] E. Vanoli, S.G. Priori, H. Nakagawa, K. Hirao, C. Napolitano, L. Diehl, R. Lazzara, P.J. Schwartz, Sympathetic activation, ventricular repolarization and I_{kr} blockade: implications for the antifibrillatory efficacy of potassium channel blocking agents, J. Am. Coll. Cardiol. 25 (1995) 1609–1614.
[14] D.J. Gallacher, A. Van de Water, H. van der Linde, A.N. Hermans, H.R. Lu, R. Towart, P.G. Volders, In vivo mechanisms precipitating torsades de pointes in a canine model of drug-induced long-QT1 syndrome, Cardiovasc. Res. 76 (2007) 247–256.
[15] R.M. ter Bekke, K.H. Haugaa, A. van den Wijngaard, J.M. Bos, M.J. Ackerman, T. Edvardsen, P.G. Volders, Electromechanical window negativity in genotyped long-QT syndrome patients: relation to arrhythmia risk, Eur. Heart J. 36 (2015) 179–186.
[16] B. Van Deuren, K. Van Ammel, Y. Somers, F. Cools, R. Straetemans, H.J. van der Linde, D.J. Gallacher, The fentanyl/etomidate-anaesthetised beagle (FEAB) dog: a versatile in vivo model in cardiovascular safety research, J. Pharmacol. Toxicol. Methods 60 (2009) 11–23.
[17] H.J. van der Linde, B. Van Deuren, Y. Somers, B. Loenders, R. Towart, D.J. Gallacher, The electro-mechanical window: a risk marker for torsade de pointes in a canine model of drug induced arrhythmias, Br. J. Pharmacol. 161 (2010) 1444–1454.
[18] P.J. Schwartz, M. Pagani, F. Lombardi, A. Malliani, A.M. Brown, A cardiocardiac sympathovagal reflex in the cat, Circ. Res. 32 (1973) 215–220.
[19] C. Lerche, G. Seebohm, C.I. Wagner, C.R. Scherer, L. Dehmelt, I. Abitbol, U. Gerlach, J. Brendel, B. Attali, A.E. Busch, Molecular impact of MinK on the enantiospecific block of I_{Ks} by chromanols, Br. J. Pharmacol. 131 (2000) 1503–1506.
[20] A. Van de Water, J. Verheyen, R. Xhonneux, R.S. Reneman, An improved method to correct the QT interval of the electrocardiogram for changes in heart rate, J. Pharmacol. Methods 22 (1989) 207–217.
[21] M.B. Thomsen, S.C. Verduyn, M. Stengl, J.D. Beekman, G. de Pater, J. van Opstal, P.G. Volders, M.A. Vos, Increased short-term variability of repolarization predicts *d*-sotalol-induced torsades de pointes in dogs, Circulation 110 (2004) 2453–2459.
[22] H.L. Tan, A. Bardai, W. Shimizu, A.J. Moss, E. Schulze-Bahr, T. Noda, A.A. Wilde, Genotype-specific onset of arrhythmias in congenital long-QT syndrome: possible therapy implications, Circulation 114 (2006) 2096–2103.
[23] S. Viskin, S.R. Alla, H.V. Barron, K. Heller, L. Saxon, I. Kitzis, G.F. Hare, M.J. Wong, M.D. Lesh, M.M. Scheinman, Mode of onset of torsade de pointes in congenital long QT syndrome, J. Am. Coll. Cardiol. 28 (1996) 1262–1268.
[24] E.Y. Birati, B. Belhassen, A. Bardai, A.A. Wilde, S. Viskin, The site of origin of torsade de pointes, Heart 97 (2011) 1650–1654.
[25] R.F. Hanich, J.H. Levine, J.F. Spear, E.N. Moore, Autonomic modulation of ventricular arrhythmia in cesium chloride-induced long QT syndrome, Circulation 77 (1988) 1149–1161.
[26] R.M. ter Bekke, P.G. Volders, Arrhythmogenic mechano-electric heterogeneity in the long-QT syndrome, Prog. Biophys. Mol. Biol. 110 (2012) 347–358.
[27] J. Han, P. Garciadejalon, G.K. Moe, Adrenergic effects on ventricular vulnerability, Circ. Res. 14 (1964) 516–524.
[28] J. Winter, A.W. Lee, S. Niederer, M.J. Shattock, Vagal modulation of dispersion of repolarisation in the rabbit heart, J. Mol. Cell. Cardiol. 85 (2015) 89–101.
[29] I. Naggar, K. Nakase, J. Lazar, L. Salciccioli, I. Selesnick, M. Stewart, Vagal control of cardiac electrical activity and wall motion during ventricular fibrillation in large animals, Auton. Neurosci. 183 (2014) 12–22.
[30] P.J. Schwartz, S.G. Priori, M. Cerrone, et al., Left cardiac sympathetic denervation in the management of high-risk patients affected by the long-QT syndrome, Circulation 109 (2004) 1826–1833.
[31] L. Crotti, C. Spazzolini, A.P. Porretta, et al., Vagal reflexes following an exercise stress test: a simple clinical tool for gene-specific risk stratification in the long QT syndrome, J. Am. Coll. Cardiol. 60 (2012) 2515–2524.
[32] A. Porta, G. Girardengo, V. Bari, A.L. George Jr., P.A. Brink, A. Goosen, L. Crotti, P.J. Schwartz, Autonomic control of heart rate and QT interval variability influences arrhythmic risk in long QT syndrome type 1, J. Am. Coll. Cardiol. 65 (2015) 367–374.
[33] M.J. Shattock, M.J. Tipton, 'Autonomic conflict': a different way to die during cold water immersion? J. Physiol. 590 (2012) 3219–3230.
[34] J. Winter, M. Tipton, M.J. Shattock, Autonomic conflict exacerbates long QT associated ventricular arrhythmia, J. Mol. Cell. Cardiol. 116 (2018) 145–154.